ELSEVIER

Biophysical Chemistry 62 (1996) 1–13

Biophysical Chemistry

Fluorescence of reduced nicotinamides using one- and two-photon excitation

Borys Kierdaszuk [a,b], Henryk Malak [a], Ignacy Gryczynski [a], Patrik Callis [c], Joseph R. Lakowicz [a,*]

[a] *Center for Fluorescence Spectroscopy, Department of Biological Chemistry, University of Maryland School of Medicine, 108 North Greene Street, Baltimore, MD 21201, USA*

[b] *Department of Biophysics, University of Warsaw, 93 Zwirki i Wigury St., PL-02089 Warsaw, Poland*

[c] *Department of Chemistry and Biochemistry, Montana State University, Bozeman, MT 59717, USA*

Received 5 July 1995; accepted 19 April 1996

Abstract

We examined the steady-state and time-resolved emission of NADH and NAMH resulting from one-photon and two-photon excitation. Similar emission spectra were observed for both modes of excitation. The fundamental anisotropy of NADH is near 0.54 for two-photon excitation from 690 to 740 nm, which is 46% higher than the value of 0.37 observed for one-photon excitation. This observation of a higher anisotropy with two-photon excitation was consistent with INDO/SDCI calculations of the one- and two-photon transitions. Minor differences in the multi-exponential decays of NADH were observed for one- and two-photon excitation, but presently available resolution does not allow us to conclude the decays are distinct. NADH-LADH-IBA complex formation led to an order of magnitude larger of the average lifetimes of NADH fluorescence resulting from one- and two-photon excitation. Fluorescence intensity and fluorescence anisotropy decays of NADH was double-exponential for both modes of excitation and show that the observed heterogeneity of the fluorescence decay kinetics of reduced nicotinamides arises from the inherent photoprocess of the dihydronicotinamide chromophore and not due to any intramolecular interactions with adenine part of NADH. Such interactions are responsible for the depolarization of NADH fluorescence observed for excitation wavelength below 300 nm for OPE and 600 nm for TPE, respectively. NADH displays a low cross-section for two-photon excitation which suggests that fluorescence from NADH will be moderately difficult to observe with two-photon fluorescence microscopy, and may not interfere with observations of TPIF of other extrinsic probes used to label cells.

Keywords: Fluorescence; Anisotropy; One-photon excitation; Two-photon excitation; Anisotropy spectra; Reduced β-nicotinamide mononucleotide; Reduced β-nicotinamide adenine dinucleotide; Time-resolved fluorescence

Abbreviations: FD Frequency-domain; FRET Fluorescence resonance energy transfer; IBA Isobutyramide; LADH Liver alcohol dehydrogenase; MSB *p*-bis(*o*-methylstyryl)benzene; β-NAD^+ β-Nicotinamide adenine dinucleotide; NADH Reduced β-Nicotinamide adenine dinucleotide; NAMH Reduced β-Nicotinamide mononucleotide; OPE One-photon excitation; OPIF One-photon induced fluorescence; PG Propylene glycol; r Steady-state fluorescence anisotropy; r_0 Limiting anisotropy in the absence of depolarizing processes; TCSPC Time-correlated single photon counting; TPIF Two-photon induced fluorescence; Tris-HCl Tris(hydroxymethyl)-aminomethane hydrochloride

* Corresponding author.

PII S0301-4622(96)02182-5

1. Introduction

Reduced nicotinamide adenine dinucleotide (NADH) is a intrinsic fluorophore present in all living systems. NADH displays an absorption maximum near 350 nm, and a structureless emission centered near 450 nm. It is known that the fluorescence intensity and quantum yield of NADH increases on binding to dehydrogenases, as described in the classic report by Velick [1]. The intrinsic emission of NADH was subsequently used to study NADH binding to lactate dehydrogenase [2], liver alcohol dehydrogenase [3] and other dehydrogenases [4,5]. The lifetime of NADH free in solution is near 0.4 ns [6,7], but the intensity decay law is at least a double exponential [8]. Upon binding to proteins the lifetime of NADH increases to 1–5 ns [3–6].

In the past two years there has been increased interest in two-photon excitation (TPE) or two-photon induced fluorescence (TPIF). By two-photon excitation we mean the simultaneous absorption of two longer wavelength photons which together result in excitation to a singlet excited state. TPE is of interest because of the possibility of larger fundamental anisotropies [9,10], resolution of overlapping transitions [11–13], and the possibility of intrinsic 'confocal' fluorescence microscopy [14]. One advantage of two-photon microscopy has been the possibility of reduced auto-fluorescence from biological samples with the use of long wavelength excitation [15].

In the present report we examined the fluorescence spectral properties of NADH when excited with two-photons of long wavelength from 570 to 740 nm. We found that NADH displays a low two-photon cross-section, suggesting that its fluorescence can be minimal in the presence of extrinsic fluorophores. The low cross-section suggests that NADH will make a minimal contribution to the emission in two-photon microscopy, particularly in the presence of extrinsic fluorophores which display higher two-photon cross sections.

2. Materials

Reduced β-nicotinamide adenine dinucleotide (NADH), disodium salt (lot no. 103H78062), and reduced β-nicotinamide mononucleotide (NAMH), sodium salt (lot no. 49f7240), were obtained from Sigma Chemical Co. Solutions were freshly prepared in 20 mM Tris-HCl buffer (pH 7.5) or in propylene glycol. The concentrations were measured spectrophotometrically as described using molar extinction coefficients of 6200 and 6400 $M^{-1} cm^{-1}$ at the absorption maxima near 340 nm [7] for solutions in water and propylene glycol, respectively.

Horse liver alcohol dehydrogenase (LADH, EC 1.1.1.1), lot number 12388822-60, was obtained from Boehringer Mannheim (Germany) as a crystalline suspension in 20 mM phosphate buffer (pH 7) containing 10% ethanol. The crystalline suspension was dissolved in an excess of 20 mM phosphate buffer (pH 7.5) and further purified with a 70% yield with repeated use of Centriprep-10 Concentrators (Amicon, Inc. Beverly, MA) to exchange buffer and to remove small molecular contaminations (mol. weight < 10 kD). These lower molecular weight species showed absorption and emission in the range 250–290 and 300–380 nm, respectively. Undissolved material was also removed by centrifugation. After desalting, the solution of LADH (~ 4 mg/ml) in 20 mM phosphate buffer (pH 7.5) was heated at 50°C for 15 min. The resulting white, flocculent precipitate (approx. 25% of protein) was removed by centrifugation [16]. Heat-treated LADH solution remained clear for at least 3 weeks at 4°C without loss of activity (3.5 U/mg), which was equivalent in that expected for the 100% pure enzyme. The concentration of LADH was measured spectrophotometrically as described using extinction coefficient of 4.55 for absorption of 1% enzyme solution at 280 nm [17]. Activity of LADH was determined by the rate of increase in absorbency at 340 nm, caused by the reduction of 8 mM β-NAD^+ to β-NADH in 10 mM sodium pyrophosphate buffer (pH 8.8) containing 0.6 M ethanol as a substrate [18]. One unit is defined as a amount of enzyme that reduces 1 micromole of NAD^+ per minute at 25°C, pH 8.8.

Propylene glycol (p.a.) was bought from Fluka Chemie AG (Buchs, Switzerland). Tris(hydroxymethyl)-aminomethane hydrochloride (made by E. Merck, Darmstadt, Germany) was purchased from E.M. Science Inc. (New Jersey, NJ). Tris-HCl buffer (pH 7.5) was made using MilliQ water and HCl (Aldrich). *p*-Bis(*o*-methylstyryl)benzene and cyclohexane (HPLC grade) were obtained from Aldrich. All other chemicals, reagents and materials were of

the highest, spectral-grade quality commercially available. They were checked by UV absorption and/or fluorescence measurements. Absorption measurements were performed on a Perkin-Elmer Lambda 6 UV/VIS spectrophotometer (The Perkin Elmer Co., Rockville, MD). Steady-state fluorescence measurements were carried out at 20 or −60°C using a SLM 8000 photon-counting spectrofluorimeter (with 2 nm spectral resolution for excitation and emission) equipped with a Hamamatsu R928 photomultiplier tube.

3. Fluorescence spectroscopic methods

Two-photon excitation was accomplished using the fundamental output of a cavity-dumped rhodamine-6G dye laser from 570 to 610 nm and/or pyridine-1 dye laser from 675 to 760 nm, which was passed through a Glan-Thompson vertical polarizer and focused in the sample using a 5 cm focal length lens. The pulse full width at half-maximum was about 5 ps at a repetition rate of 3.795 MHz. One-photon induced fluorescence and excitation anisotropy spectra were measured using the same laser system as for two-photon induced fluorescence equipped additionally with a 390 frequency doubler (Spectra Physics) and a polarization rotator. For reliable comparison of the fluorescence and excitation anisotropy spectra resulting from these two types of excitation we used an instrument for time-correlated single photon counting (TCSPC) [19,20]. The steady-state intensity at each wavelength was obtained by integrating the time-resolved intensity measurements. In addition to increased sensitivity, the use of TCSPC allowed us to demonstrate the absence of scattered light in the detected emission by the absence of components with the same time profile as the excitation pulse.

For two-photon experiments we used 1.0 × 0.5 cm cuvettes placed in the thermostated SLM cell holder (Urbana, Champaign, IL), with a long axis aligned along the incident light path and with the focal point positioned about 0.5 cm from the surface facing the incident light. The position of the cuvette and the lens were adjusted so that the focal point of the laser excitation was located closest to the observation window. For one-photon experiments we used 0.5 × 0.5 cm cuvettes in the 1 × 1 cm cuvette holder and with an excitation and emission positioned near a cuvette corner, which practically eliminated trival reabsorption occurring for a longer path length. Fluorescence was collected by a suprasil lens, filtered from the contaminating scatter of the long-wavelength light using Corning 3-73 and 4-96 filters (2 and 5 mm thick) and passed through an ISA (New Jersey) grating monochromator (4 nm slit bandwidth) and Glan-Thompson polarizer in the magic angle position. The wavelength scale of the monochromator was calibrated using a SCT1 mercury lamp (Ultra-Violet Products Inc., San Gabriel, CA) as a wavelength standard. Fluorescence spectra were corrected for transmittance of the filters used to isolate the emission. The effect of the intensity of incident light on the one-photon and two-photon induced fluorescence intensity (Figs. 1 and 2, inserts) was measured using neutral density filters to decrease the peak excitation intensity. Signal from the solvent alone was less than 0.5% and was subtracted from sample fluorescence.

For anisotropy determinations, the polarized emission was observed through an interference filter cen-

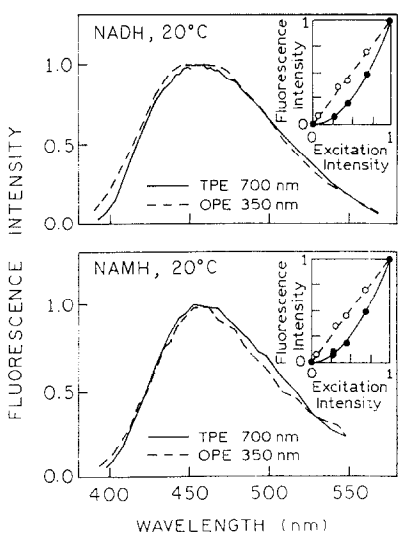

Fig. 1. Fluorescence emission spectra of NADH (top) and NAMH (bottom) in 20 mM Tris-HCl (pH 7.5) at 20°C obtained for one (- - - -) and two photon (—) excitation. The inserts shows the dependence of the one-photon (- - o - -) and two-photon induced fluorescence intensity (—●—) on the intensity of the 350 (O) or 700 nm (●) incident light. The maximum intensities for OPE and TPE are both normalized to unity in the spectra and the inserts.

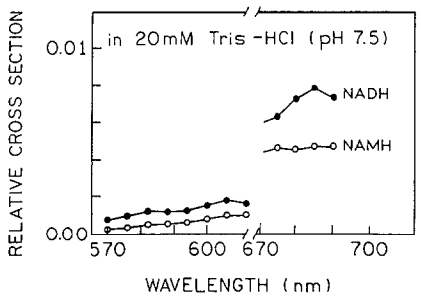

Fig. 2. Wavelength-dependent two-photon cross section of 1 mM NADH (—●—) and 1 mM NAMH (- - o - -) in 20 mM Tris-HCl (pH 7.5) at 20°C. The cross sections are measured relative to 0.16 mM MSB in cyclohexane. The cross sections are normalized to the two-photon cross section of MSB at the same wavelengths.

tered at 460 nm (10 nm band-pass), a Glan-Thompson polarizer and two Corning filters 3-73 and 4-96. The anisotropy, r, values were determined from the polarized fluorescence intensities as

$$r = (gF_{vv} - F_{vh})/(gF_{vv} + 2F_{vh}) \quad (1)$$

where F_{vv} is vertically polarized emission intensity with vertically polarized excitation, and F_{vh} is horizontally polarized emission with vertically polarized excitation. The instrumental correction factor, g, is equal to $g = F_{hh}/F_{hv}$, where F_{hh} is horizontally polarized emission intensity with horizontally polarized excitation, and F_{hv} is vertically polarized emission with horizontally polarized excitation. This g factor corrects for the small polarization bias of the optical system and photomultiplier. The g factor was usually within a few percent of 1.0. Anisotropy values presented here were checked by an independent determination at 285, 300, 350 and 374 nm for OPE and at 570, 600, 700 and 748 nm for TPE.

Frequency-domain intensity and anisotropy decays were obtained on the GHz instrument [21,22] using one- and two-photon excitation at 350 and 700 nm, respectively, as described above for the steady state measurements. Data were analyzed as described previously [23–25]. Intensity decays $I(t)$ were fit to the multi-exponential model using

$$I(t) = \sum_i \alpha_i \exp(-t/\tau_i) \quad (2)$$

where α_i are the amplitudes associated with the decay time τ_i. The fractional intensity decay f_i is given by $f_i = \alpha_i\tau_i/\Sigma_j\alpha_j\tau_j$ and mean decay time $\langle\tau\rangle$ is given by $\langle\tau\rangle = \Sigma_i f_i\tau_i$.

The differential phase and modulated anisotropy data were fit to multiexponential anisotropy decay ($r(t)$) model using

$$r(t) = \sum_j r_{oj} \exp(-t/\theta_j) \quad (3)$$

where r_{0j} is the amplitude which decays with a correlation time θ_j. The total anisotropy is given by $r_0 = \Sigma r_{0j}$. For analysis of the intensity decays the uncertainties in phase and modulation were assumed to be 0.4° and 0.01, respectively. For analysis of the anisotropy decays the same uncertainties were assumed for the differential polarized phase and modulation ratios, respectively.

Time-domain intensity decays were measured using the same experimental apparatus used for the steady state measurements. The intensity decays $I(t)$ were fit to the multi-exponential model (Eq. (2)).

4. Results

4.1. One- and two-photon induced emission of NADH and NAMH

It is well known that emission spectra of NADH and NAMH are not identical, the NAMH spectrum appears to be red shifted about 3 nm [8]. Hence, it was of interest to determine whether the two-photon induced emission spectrum of NADH and NAMH displayed a similar difference. Emission spectra of NADH (Fig. 1, top) and NAMH (Fig. 1, bottom) in 20 mM Tris-HCl buffer (pH 7.5) are shown for OPE at 350 and TPE at 700 nm. For direct comparison, the OPE spectra were recorded on the same instrument as for TPE spectra (see Materials and Methods), except for the use of a frequency doubler for OPE. For one-photon excitation at 350 nm the emission intensity is linear proportional (Fig. 1, inserts) to the intensity of the 350 nm incident light (- o -). In contrast, for TPE at 700 nm, the intensity is dependent on the square of the peak laser power (- ● -). The quadratic dependence on the excitation intensity demonstrates that the observed emission is due to a biphotonic process at 700 nm. The emission spectra of NADH and NAMH appear to be essentially simi-

lar for OPE and TPE (Fig. 1). We do not think that the minor spectral differences seen at 430 nm for NADH and 500 nm for NAMH are experimentally significant. The two-photon induced fluorescence spectrum of NAMH is also red shifted, as was observed for one-photon induced fluorescence. These results suggest that the emission occurs from the same electronic state for both one-photon and two-photon excitation.

4.2. Two-photon cross sections for NADH and NAMH

There is presently considerable interest in the use of two-photon induced fluorescence in microscopy and/or cellular imaging [14,15]. This interest arises from the possibility of obtaining improved Z-axis resolution because the use of TPIF results in intrinsic 'confocal' excitation. TPIF is spatially localized at the focal plan due to its quadratic dependence on light intensity. Hence, out-of-plane fluorescence is excited to a lesser extent than for one-photon fluorescence microscopy.

In fluorescence microscopy, the emission from reduced NADH and its analogues is the main source of auto-fluorescence with UV excitation. Hence it is of interest to determine the cross section for TPIF of NADH, as this will indicate the extent to which NADH will contribute to the auto-fluorescence in two-photon microscopy and the usefulness of NADH as an intrinsic probe for TPIF.

Since the extent of two-photon absorption is weak, it is difficult to directly measure two-photon cross sections. Hence, we examine TPIF of NADH and NAMH relative to *p*-bis(*o*-methylstyryl)benzene (MSB) in cyclohexane as a standard for two-photon excitation spectra [26]. For each excitation wavelength we measured TPIF of 1 mM NADH and NAMH in 20 mM Tris-HCl buffer (pH 7.5), and 0.16 mM MSB in cyclohexane, as well as background fluorescence from 20 mM Tris-HCl buffer (pH 7.5) and cyclohexane. Fluorescence from the solvents alone were subtracted from the sample fluorescence. The two-photon cross section spectra for NADH and NAMH were calculated relative to MSB and are presented in Fig. 2 for the two spectral ranges available on our laser systems (see Materials and Methods). The long-wavelength range was additionally limited by the available two-photon cross section data for MSB, which are limited to excitation wavelengths lower than 695 nm [26]. In the long-wavelength excitation range from 675 to 690 nm the two-photon cross section for NADH is approximately 100-fold lower than for MSB. The two-photon cross section for NAMH is 1.6-times lower than for NADH, which is similar to the relation between their quantum yields obtained for one-photon excitation [8]. In the short-wavelength range from 570 to 610 nm we observed a 5-fold lower cross section for both analogues, with the ratio between them being somewhat dependent on the excitation wavelength. The ratio of cross sections for NADH relative to NAMH increases from 1.8 at 600–610 nm to 2.8 at 570–580 nm. This wavelength dependence of the relative cross section may coincide with the adenine absorption at 261 nm, so it seems possible that the larger two-photon cross section of NADH is caused by a radiationless energy transfer from the adenine to nicotinamide. Energy transfer from adenine to nicotinamide seems to be responsible for a strong depolarizing effect observed in the excitation anisotropy spectra observed for one- and two-photon excitation of free NADH and in the complex with LADH (below).

4.3. Excitation anisotropy spectra of NADH, NAMH and NADH-LADH-IBA complex

In previous studies of TPIF we observed that the fundamental anisotropy (r_0) observed in the absence of depolarizing rotational diffusion is sometimes larger for TPIF than for OPIF[9,10], whereas in the case of indole, tryptophan [13], phenol and tyrosine [27] the r_0 values are lower for TPIF than for OPIF. Hence, we examined the excitation anisotropy spectra of NADH and NAMH in vitrified solution (Fig. 3). The TPIF excitation anisotropy spectra could only be obtained for a limited range of wavelengths, where output intensities obtained from our Rhodamine 6G and Pyridine-1 dye lasers provided an adequate fluorescence signal. In the long-wavelength range the anisotropy values for TPE of NADH and NAMH were found to be 0.540 ± 0.005 and 0.537 ± 0.006, while anisotropy for OPE was 0.370 ± 0.002 and 0.368 ± 0.004, respectively. These values appear to be related by the photoselection factor 10/7, which is caused by an apparent $\cos^4\Theta$ photoselec-

tion for TPE and $\cos^2\Theta$ for OPE. This result indicates that the electronic transitions for absorption and emission are nearly co-linear for both OPE and TPE, and suggests that the one-photon and two-photon transitions have the same orientation in the molecular axis. In the short-wavelength range from 590 to 610 nm the anisotropies also appear to be related by the factor 10/7. At shorter wavelengths from 560 to 590 nm the NADH anisotropy values are smaller than for NAMH, for which the anisotropy values remain constant for both modes of excitation (Fig. 3).

Because of the low two-photon cross sections of the reduced nicotinamide it was necessary to use relatively high concentrations of 0.5 mM to obtain the excitation anisotropy spectra in Fig. 3. Hence we questioned whether the observed values were affected by fluorescence resonance energy transfer. To obtain the excitation anisotropy spectrum in the absence of FRET we examined the anisotropy for OPE of 20 μM NADH and NAMH in vitrified solution using a steady state spectrofluorometer for the 260–400 nm range (Fig. 4). We observed comparable OPE anisotropy values in this dilute solution (Fig. 4) as observed in the more concentrated samples used for TPE. This result suggest that FRET was not a significant factor in the TPE anisotropy spectra. The NADH anisotropy decreased dramatically when excitation wavelength decreased to 275 nm, confirming the wavelength dependence of the NADH anisotropy measured on the laser system for OPE at 285–295 nm and for TPE at 570–600 nm (Fig. 3).

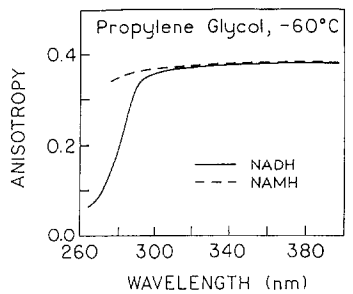

Fig. 4. One-photon excitation anisotropy spectra of 20 μM NADH (—) and 20 μM NAMH (- - -) in propylene glycol at −60°C measured for the emission at 460 nm.

To further examine the possibility of FRET and/or complex formation among the nucleotides we examined NADH and NAMH in solutions of increasing concentration (Fig. 5). We examined the effect of concentration of the anisotropy values for OPE and TPE of NADH and for OPE of NAMH (Fig. 5). The anisotropy values were essentially constant up to 3 mM, which is a 6-fold higher concentration than used to obtained the anisotropy spectra. These results suggest that the anisotropy spectra of NADH and NAMH (Fig. 3) are not affected by an intermolecular energy transfer or complex formation between fluorophores.

While high concentrations of NADH and NAMH were used for the two-photon anisotropy spectra, this may not be needed in two-photon microscopy. For microscopic imaging it is now standard practice to use fs pulses from Ti:Sapphire lasers, which can provide higher peak powers that are available from

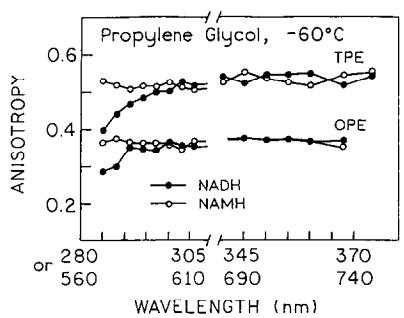

Fig. 3. Excitation anisotropy spectra of 0.5 mM NADH (—●—) and 0.5 mM NAMH (—o—) in propylene glycol at −60°C measured for emission at 460 nm, for one and two-photon excitation.

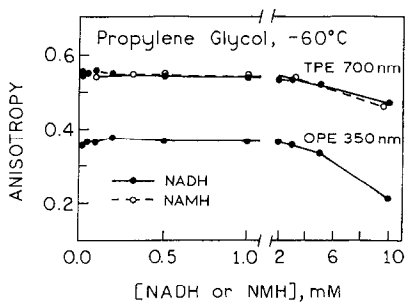

Fig. 5. Concentration dependence of the fluorescence anisotropy of NADH (—●—) and NAMH (—o—) in propylene glycol at −60°C measured for the emission at 460 nm, for one and two-photon excitation.

our ps dye lasers. Also, the focusing can be superior with the microscope optics, so that much lower concentrations of NADH will be observable in two-photon microscopy.

We next examined the anisotropy of 20 μM NADH in the ternary complex with 20 μM LADH and 100 mM isobutyramide (IBA) in 20 mM Tris-HCl (pH 7.5) at 20°C, where concentrations of NADH, LADH and IBA were optimal for almost 100% binding of NADH to LADH [28,29]. The data for OPE in the 310–400 nm range displayed about 3-fold larger anisotropy values for NADH in the ternary complex than for 20 μM NADH in 20 mM Tris-HCl (pH 7.5), and 10%–20% larger than anisotropy of 20 μM NADH in propylene glycol at 20°C (Fig. 6). These anisotropy spectral show a wavelength-dependent depolarization in the 260–310 nm range. The depolarization observed in the anisotropy spectrum for TPE of NADH-LADH-IBA complex in 20 mM Tris-HCl at 20°C (Fig. 7) is larger than for OPE of this complex. In the long-wavelength range the anisotropy values are related by photoselection factor of 10/7, while in the short-wavelength range this relation is not valid and anisotropy for TPE is even lower than for OPE. These results indicate the presence of another depolarizing factor caused by a simultaneous two-photon excitation of LADH fluorophores in the NADH-LADH-IBA complex. It seems likely that the decrease of the NADH anisotropy is caused by radiationless energy transfer from trytophan and/or ionized tyrosine residues to NADH (see Discussion section).

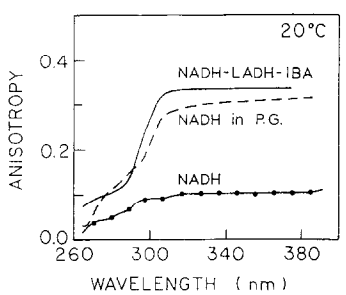

Fig. 6. Excitation anisotropy spectra of 20 μM NADH in 20 mM Tris-HCl (pH 7.5) (-●-●-), in propylene glycol (- - -) and with 20 μM LADH and 100 mM IBA (—) in 20 mM Tris-HCl (pH 7.5) for one-photon excitation at 20°C.

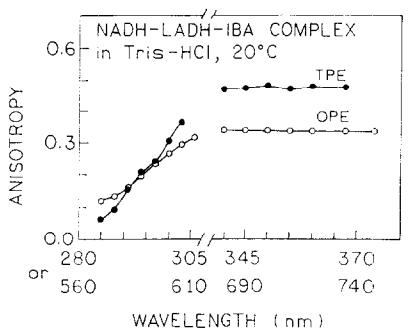

Fig. 7. Excitation anisotropy spectra for the mixture of 20 μM NADH, 20 μM LADH and 100 mM IBA in 20 mM Tris-HCl (pH 7.5) at 20°C obtained for emission at 460 nm and for one-photon (—o—) and two-photon excitation (—●—).

4.4. Theoretical predictions of TPIF

Given the unsymmetrical nature of the nicotinamide chromophore, we must rely upon semiempirical molecular orbital methods for an understanding of the observed anisotropy observed under two-photon excitation. Here we use the INDO/SDCI [30] method which has been moderately successful for predicting two-photon properties, [31] including TPIF [32]. As in other applications to two-photon spectra, two parameter sets were used: 1) SCI, involving only singly excited configurations and using Mataga-Nishimoto electron repulsion. 2) SDCI, involving singly and doubly $\pi\pi^*$ excitations, and using Ohno-Klopman electron repulsion. The latter more properly treats certain types of states, e.g., the two-photon allowed A_g states of linear polyenes, and gives more accurate two-photon absorptivities. Computations were performed only for the chromophoric part of NAMH, i.e., a hydrogen replaced the ribose attachment. The geometry used for NAMH model was optimized using the AM1 option of MOPAC6.

For this molecule the SCI and SDCI computations gave very similar results. In both cases, the lowest transition was predicted to be primarily HOMO → LUMO, and to have an oscillator strength of 0.15. The SCI transition wavelength maximum of 345 nm, is in good agreement with experiment. The SDCI transition wavelength maximum was 300 nm, a typical underestimate for this method. Both methods predict two-photon crossections which are fairly strong, about 10 times stronger than for the ^1L_a transition of tryptophan.

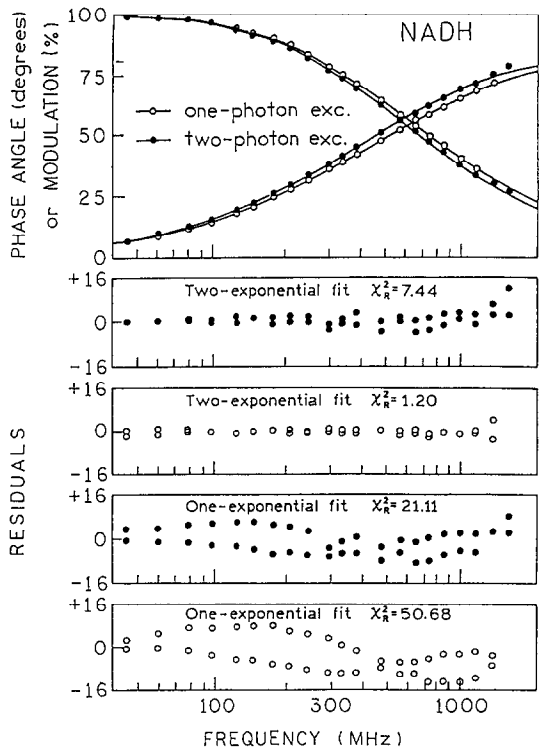

Fig. 8. Frequency-domain intensity decays of 1 mM NADH in 20 mM Tris-HCl (pH 7.5) at 20°C obtained for OPE 350 nm (—o—) and for TPE 700 nm (—●—). The solid lines represent the best fits obtained for double-exponential model with lifetimes and amplitudes shown in Table 1. The bottom panels show the weighted residuals obtained for the one- and two-exponential fits and for one-photon (o) and two-photon excitation (●). The residuals are relative to the assume uncertainities.

In both cases, the two-photon tensor is primarily composed of a single element when the principal axis vector points from the oxygen to the ring nitrogen. This coincides almost exactly with the direction of the one-photon transition dipole computed in both cases. As a result, the TPIF anisotropy is predicted to be very high ($r = 0.59$) in both types of computation. It is predicted to be higher than the nominal maximum value of 4/7 (0.57) because of small negative lobes in the tensor, which have been shown to cause the theoretical TPIF anisotropy to be as high as 0.6123 [32].

The highest experimental value of the TPIF anisotropy found in this work for NAMH is 0.54, i.e., about as high as any experimental value ever reported. The deviation of this value from the predicted value of 0.59 is not considered significant at this time. The value is well within the accuracy expected from the theory, and experimental values tend to fall below theoretical values even when done with extreme care.

It is of passing interest to examine the reason for near colinearity of the tensor and transition dipole. The computation reveals that the main term arises from the product of the large transition dipole and the large change in permanent dipole moment (~ 5 Debye) accompanying the transition. The transition transfers electron density from the ring N towards the amide group. This is the same mechanism which accounts for the high TPIF anisotropy of POP [32].

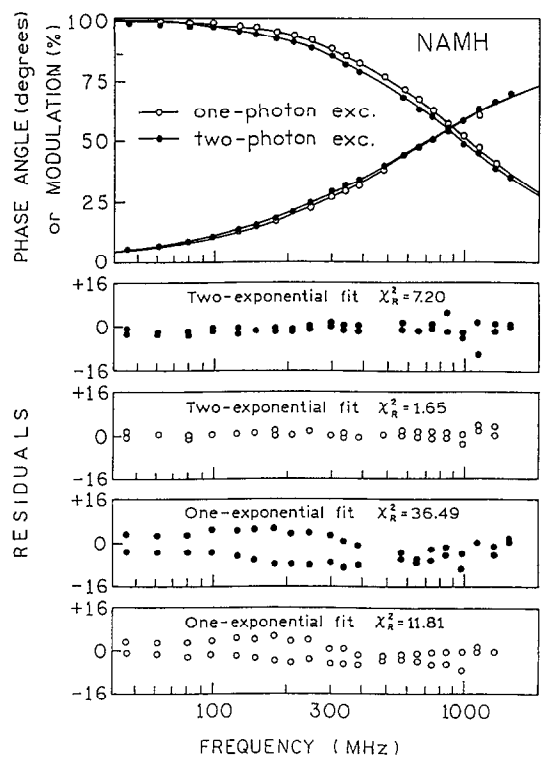

Fig. 9. Frequency-domain intensity decays of 1 mM NAMH in 20 mM Tris-HCl (pH 7.5) at 20°C obtained for OPE 350 nm (—o—) and for TPE 700 nm (—●—). The solid lines represent the best fits obtained for double-exponential model with lifetimes and amplitudes shown in Table 1. The bottom panels show the weighted residuals obtained the for one- and two-exponential fits and for one-photon (o) and two-photon excitation (●). The residuals are relative to the assume uncertainities.

Next, we comment on the short wavelength anisotropy in the region of the adenosine absorption band. The 260 nm band of 9-methyladenine is known to have two $\pi\pi^*$ transition, similar to trytophan. Unlike trytophan, the two moments are nearly parallel, being only about 25° apart in direction [33]. The drop in anisotropy seen for NADH as the excitation wavelength is changed to 285 n suggests that the adenine transition dipoles are not optimally parallel to the nicotinamide transition dipole. Not much more can be said because the data do not extend to the adenine maximum. INDO/S computations on 9-methyladenine indicate that the main two-photon intensity has a tensor direction nearly perpendicular to the one-photon transition dipoles[34]. Therefore there should be an inverse relation between the depolarization seen for one- and two-photon excitation. That they show similar depolarization suggests that the angle between the adenine and nicotinamide transition moments is about 45°. For the NADH-LADH-IBA complex, where the TPIF anisotropy drops more steeply, it may be that the angle is smaller. It is also possible that two-photon excitation is more efficient to other chromophores in the LADH which depolarize by energy transfer.

4.5. Fluorescence intensity and anisotropy decay of NADH, NAMH and NADH-LADH-IBA complex

Frequency responses for the NADH and NAMH emission at 460 nm and for OPE 350 nm and TPE 700 nm are shown in Figs. 8 and 9. We observed double-exponential decays for NADH and NAMH for 350 nm excitation and 460 nm emission. The data were well fit using the double exponential model. The triple-exponential analysis did not result in a decrease in χ^2_R. While the short component of NAMH fluorescence has the same lifetime for both modes of excitation, TPE of NADH resulted with a larger lifetime than OPE (Table 1). For both analogs, the average lifetimes are larger for TPE than for OPE. At this time we do not think that small difference in the component lifetimes of one- and two-photon induced fluorescence are significant, and the presence or absence of small differences in the intensity decay can only be decided by further experimentation. The values of χ^2_R are larger for TPE than for OPE because the emission is weaker for TPH and consequently the random error is larger.

The frequency-domain intensity data for 20 μM NADH, its mixture with 20 μM LADH and 100 mM

Table 1
Multi-exponential analysis of the fluorescence intensity decays resulting from OPE 350 nm and TPE 700 nm of NADH, NAMH and ternary complex, NADH-LADH-IBA [a]

Compound	Excitation (nm)	α_i	f_i [b]	τ_i (ns)	$\langle\tau\rangle$ [c] (ns)	χ^2_R 1exp	χ^2_R 2exp.
NAMH	350	0.970	0.914	0.251			
		0.030	0.086	0.760	0.294	11.81	1.65
	700	0.962	0.878	0.255			
		0.038	0.122	0.904	0.334	36.49	7.20
NADH	350	0.717	0.537	0.270			
		0.283	0.463	0.590	0.418	50.68	1.20
	700	0.933	0.851	0.373			
		0.067	0.149	0.909	0.453	21.11	7.44
NADH-LADH	350	0.120	0.022	0.684			
-IBA		0.880	0.978	4.075	4.000	14.2	1.1

[a] Fluorescence intensity decays were measured for 1 mM solutions of free NAMH and free NADH in 20 mM Tris-HCl buffer (pH 7.5) at 20°C using frequency-domain fluorometry and experimental condition described in Section 2. Ternary complex, NADH-LADH-IBA, was obtained in solution of 20 μM NADH, 20 μM LADH and 100 mM IBA in 20 mM Tris-HCl buffer (pH 7.5) at 20°C. [b] $f_i = \alpha_i\tau_i/\Sigma_j\alpha_j\tau_j$. [c] $\langle\tau\rangle = \Sigma_i f_i\tau_i$.

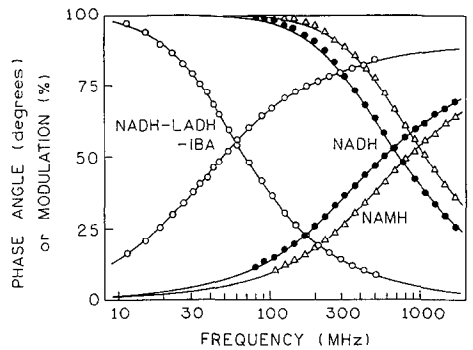

Fig. 10. Frequency-domain intensity decays of 20 μM NAMH (△), 20 μM NADH (●) and its mixture with 20 μM LADH and 100 mM IBA (O) in 20 mM Tris-HCl (pH 7.5) at 20°C obtained for excitation at 350 nm. The solid lines represent the best fits obtained for double-exponential model with lifetimes and amplitudes shown in Table 1.

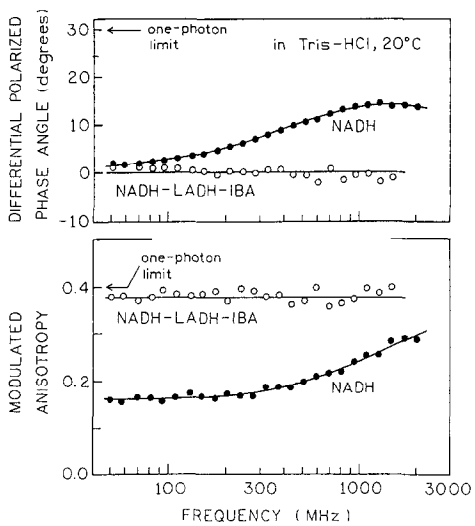

Fig. 11. Frequency-domain anisotropy data for the emission of 20 μM NADH in 20 mM Tris-HCl (pH 7.5) (●), and its mixture with 20 μM LADH and 100 mM IBA (O) in 20 mM Tris-HCl (pH 7.5) at 20°C obtained for excitation at 350 nm. The best fit with two correlation times ($\theta_1 = 0.13$ and $\theta_2 = 1.10$ ns) and $\chi^2_R = 1.8$ is represented by the solid line for NADH alone. The solid line for the sample containing LADH represents an approximate fit of the experimental results.

IBA and for 20 μM NAMH in 20 mM Tris-HCl (pH 7.5) are presented in Fig. 10. For NADH in the ternary complex, NADH-LADH-IBA, a double-exponential decay was also observed for OPE at 350 nm by frequency-domain fluorometry (Table 1) as well as by time-domain techniques for OPE 350 nm and TPE 700 nm (Table 2). The triple-exponential analysis did not result in a decrease in χ_R. Ternary complex formation led to a 10-fold larger average lifetime of NADH fluorescence (Fig. 10, Tables 1 and 2) with the fractional intensities strongly dominated by the long component. The short component of NADH fluorescence in the ternary complex has a lifetime much larger than an average lifetime for free NADH in aqueous solution (Table 1).

The anisotropy decays of NADH free in solution and in the ternary complex are shown in Fig. 11. The frequency-domain anisotropy data are similar for

Table 2
Multi-exponential analysis of the fluorescence intensity decays of NADH resulting from OPE 350 nm and TPE 700 nm of the ternary complex, NADH-LADH-IBA [a]

Excitation (nm)	α_i	f_i [b]	τ_i (ns)	$\langle\tau\rangle$ [c] (ns)	χ^2_R 1exp	χ^2_R 2exp.
OPE 350 nm	0.321	0.036	0.341			
	0.679	0.964	4.352	4.208	1.26	1.00
TPE 700 nm	0.402	0.050	0.371			
	0.598	0.950	4.737	4.519	1.45	1.12

[a] Fluorescence intensity decays of NADH in the ternary complex were measured for the mixture of 20 μM NADH, 20 μM LADH and 100 mM IBA in 20 mM Tris-HCl buffer (pH 7.5) at 20°C using time-correlated single photon counting method and experimental condition described in Section 2. [b] $f_i = \alpha_i\tau_i / \Sigma_j \alpha_j\tau_j$. [c] $\langle\tau\rangle = \Sigma_i f_i\tau_i$.

Table 3
Anisotropy decay analysis of 20 μM NADH and NAMH fluorescence in 20 mM Tris-HCl buffer (pH 7.5) at 20C [a]. Anisotropy decays were measured using frequency-domain fluorometry with 350 m excitation and 460 nm emission

Compound	r_{oj} [b]	θ_j [b] (ns)	χ^2_R 1exp.	χ^2_R 2exp.
NAMH	0.09(0.03)	1.2(0.5)		
	0.29(0.03)	0.13(0.01)	11.1	2.5
NADH	0.14(0.02)	1.1(0.3)		
	0.24(0.02)	0.13(0.01)	13.2	1.8

[a] Standard deviation values (in brackets) represent the 67% confidence intervals. [b] The r_{oj} is the amplitude of the anisotropy which decays with a correlation time θ_j, and the total anisotropy r_o is given by ($r_o = \Sigma_j r_{oj}$).

OPE of NADH and NAMH (Table 3). We observed a double-exponential anisotropy decays for NADH and NAMH for excitation at 350 nm and emission at 460 nm with similar correlation times. The amplitude associated with a short correlation time is larger for NAMH, which could be explained by lower molecular weight and different molecular shape as compare as with NADH [35]. The fluorescence anisotropy decay of NADH from the ternary complex, NADH-LADH-IBA, was not measurable within a time-scale of the average fluorescence lifetime of NADH. This is due to a very large correlation time associated with a slow rotational diffusion of the ternary complex, which is much larger than the average lifetime of NADH fluorescence. The differential phase and modulation do not show any dependance on the modulation frequency (Fig. 11). Hence, the accurate determination of the correlation time for ternary complex based on the NADH fluorescence is impossible.

5. Discussion

This article compares the fluorescence of NADH resulting from one- and two-photon excitation. NADH was examined free in aqueous solution and bound to the active center of LADH in the ternary NADH-LADH-IBA complex. The results show that the same emission spectra of NADH and NAMH are observed for OPE and TPH. The two-photon cross sections for NADH and NAMH are rather small, suggesting that these nucleotides will display weak signals in two-photon microscopy. The limiting anisotropy (r_0) values are related by the photoselection factor 10/7 which can be explained by $\cos^2 \theta$ and $\cos^4 \theta$ photoselection for OPE and TPE, respectively. Additionally, INDO/SDCI calculations suggest a single element for the two-photon transition tensors, which is consistent with the one- and two-photon anisotropies.

The intensity decays of NADH and NAMH are both heterogeneous and best fits were obtained using a double exponential model for both OPE and TPE. The multi-exponential decay parameters were slightly different for OPE and TPE, with slightly longer lifetimes for TPE. However, these differences are minor, and cannot be regarded as definite without further experimentation. The same double exponential model describes the NADH fluorescence decays of the ternary NADH-LADH-IBA complex although an average lifetimes were an order of magnitude larger. This results further confirm the heterogeneity of the fluorescence decay kinetics of reduced nicotinamides observed for one-photon excitation [8,36] which arises from the inherent photoprocess of the dihydronicotinamide chromophore which is independent on the mode of excitation and not due to any intramolecular interactions [35] as assumed earlier [8].

The LADH binding on NADH fluorescence was usually attributed to a tryptophan-NADH energy transfer [37], but Lowes and Shore [38,39] argued that it could be due neither to FRET nor to collisional quenching by virtue of the fact that the tryptophan residues are far from the active center of the enzyme [40]. As a result of the large conformational changes of LADH in the presence of coenzyme tryptophan-314 does not change its environment while tryptophan-15 is reported to become more exposed to the solution. Hence, Lowes and Shore [38] postulated that ternary complex formation causes a ionization of tyrosine-286 at the surface of the enzyme. They further suggested that ionized tyrosine could be acceptor of the resonance energy from trp-314. Perhaps, ionized tyrosine could also be an energy donor for NADH, but there is no evidence for such possibility. Furthermore, NADH fluorescence could be affected by conformational changes of coenzyme molecule due to the complex formation with LADH [40]. In fact, we showed here the effect of ternary complex formation on the anisotropy of NADH fluorescence which could be explained by both phenomena.

Acknowledgements

This work was supported by grant No. RR-08119 from National Institutes of Health, and by grant No. MCB-8804931 from the NSF; and in part by grants UM-141 and HMI 75195-543401 (University of Warsaw, Poland). Dr. Borys Kierdaszuk is indebted to the Fulbright Scholar Program for Advanced Research Grant.

References

[1] S.F. Velick, Fluorescence Spectra and Polarization of Glyceraldehyde-3-phosphate and Lactic Dehydrogenase Coenzyme Complexes. J. Biol. Chem., 233 (1958) 1455–1467.

[2] S.R. Anderson and G. Weber, Multiplicity of Binding by Lactate Dehydrogenases. Biochem., 4 (1965) 1948–1957.

[3] A. Gafni and L. Brand, Fluorescence Decay Studies of Reduced Nicotinamide Adenine Dinucleotide in Solution and Bound to Liver Alcohol Dehydrogenase, Biochem., 15 (1976) 3165–3171.

[4] J.C. Brochon, P. Wahl, M. Monneuse-Doublet and A. Olomucki, Pulse Fluorimetry Study of Octopine Dehydrogenase-Reduced Nicotinamide Adenine Dinucleotide Complexes, Biochem., 16 (1977) 4594–4540.

[5] J.C. Brochon, P. Wahl, J-M. Jallon and M. Iwatsubo, Pulse Fluorimetry Study of Beef Liver Glutamate Dehydrogenase-Reduced Nicotinamide Adenine Dinucleotide Phosphate Complexes, Biochem., 15 (1976) 3259–3265.

[6] J.R. Lakowicz, H. Szmacinski, K. Nowaczyk and M.L. Johnson, Fluorescence Lifetime Imaging of Free and Protein-Bound NADH, Proc. Nat. Acad. Sci., 89 (1992) 1271–1275.

[7] T.G. Scott, R.D. Spencer, N.J. Leonard and G. Weber, Emission Properties of NADH. Studies of Fluorescence Lifetimes and Quantum Efficiencies of NADH, AcPyADH, and Simplified Synthetic Models, J. Am. Chem. Soc., 92 (1970) 687–695.

[8] A.J.W.G. Visser and A. Van Hoek, The Fluorescence Decay of Reduced Nicotinamides in Aqueous Solution after Excitation with a UV-Mode Locked Ar Ion Laser, Photochem. Photobiol., 33 (1981) 35–40.

[9] J.R. Lakowicz and I. Gryczynski, Fluorescence Intensity and Anisotropy Decay of 4',6-Diamidino-2-phenylindole-DNA Complex Resulting from-39 One-Photon and Two-Photon Excitation, J. Fluoresc., 2 (1992) 117–121.

[10] J.R. Lakowicz, I. Gryczynski, Z. Gryczynski, E. Danielsen and M.J. Wirth, Time-Resolved Fluorescence Intensity and Anisotropy Decays of 2,5-Diphenyloxazole by Two-Photon Excitation and Frequency-Domain Fluorometry, J. Phys. Chem., 96 (1992) 3000–3006.

[11] R.R. Birge, L.P. Murray, B.M. Pierce, H. Akita, V. Balogh-Nair, L.A. Findsen and K. Nakanishi, Proc. Natl. Acad. Sci. USA 82, (1985) 4117–4121.

[12] R.R. Birge, Two-photon Spectroscopy of Protein-Bound Chromophores, Acc. Chem. Res., 19 (1986) 138–146.

[13] J.R. Lakowicz, I. Gryczynski, E. Danielsen and J. Frisoli, Anisotropy Spectra of Indole and N-acetyl-L-tryptophanamide Observed for Two-photon Excitation of Fluorescence, Chem. Phys. Lett., 194 (1992) 282–287.

[14] W. Denk, J.H. Strickler and W.W. Webb, Two-photon Excitation in Laser Scanning Microscopy, Science, 248 (1990) 73–76.

[15] D.W. Piston, D.R. Sandison and W.W. Webb, Time-resolved Fluorescence Imaging and Background Rejection by Two-Photon Excitation in Laser Scanning Microscopy, SPIE, 1640 (1992) 379–388.

[16] M.R. Eftink and L.A. Selvidge, Fluorescence Quenching of Liver Alcohol Dehydrogenase by Acrylamide, Biochem., 21 (1982) 117–125.

[17] D.J. Cannon and R.H. McKay, The Amino Acid Composition of Horse Liver Alcohol Dehydrogenase, Biochem., 6 (1969) 3510–3514.

[18] B.L. Valle and F.L. Hoch, Zinc, a Component of Yeast Alcohol Dehydrogenase, Proc. Natl. Acad. Sci., 41 (1955) 327–329.

[19] D.V. O'Connor and D. Philips, Time-Correlated Single Photon Counting, Academic Press, London, 1984.

[20] D.J.S. Birch and R.E. Imhof, Time-Domain Fluorescence Spectroscopy Using Time-Correlated Single-Photon Counting, in J.R. Lakowicz, (Ed.) Topics in Fluorescence Spectroscopy, Vol: 1, Techniques, Plenum, New York, (1991) pp. 1–95.

[21] J.R. Lakowicz, G. Laczko and I. Gryczynski, A 2 GHz Frequency-Domain Fluorometer, Rev. Sci. Instrm., 57 (1986) 2499–2506.

[22] G. Laczko, J.R. Lakowicz, I. Gryczynski, Z. Gryczynski and H. Malak, A 10 GHz Frequency-Domain Fluorometer, Rev. Sci. Instrum., 61 (1990) 2331–2337.

[23] J.R. Lakowicz, E. Gratton, G. Laczko, H. Cherek and M. Limkeman, Analysis of Fluorescence Decay Kinetics from Variable-Frequency Phase Shift and Modulation Data, Biophys. J., 46 (1984) 463–477.

[24] E. Gratton, J.R. Lakowicz, B. Maliwal, H. Cherek, G. Laczko and M. Limkeman, Resolution of Mixtures of Fluorophores Using Variable-Frequency Phase and Modulation Data, Biophys. J., 46 (1984) 479–486.

[25] B.P. Maliwal and J.R. Lakowicz, Resolution of Complex Anisotropy Decays by Variable Frequency Phase-Modulation Fluorometry: A Simulation Study, Biochim. Biophys. Acta., 873 (1986) 162–172.

[26] S.M. Kennedy and F.E. Lytle, *p*-Bis(*o*-methylstyryl)benzene as a Power-Squared Sensor for Two-Photon Absorption Measurements Between 537 and 694 nm, Anal. Chem., 58 (1986) 2643–2647.

[27] J.R. Lakowicz, B. Kierdaszuk, P. Callis, H. Malak and I. Gryczynski, Fluorescence Anisotropy of Tyrosine Using One- and Two-Photon Excitation, Biophy. Chem., 56 (1995) 263–271.

[28] A. Gafni and L. Brand, Fluorescence Decay Studies of Reduced Nicotinamide Adenine Dinucleotide in Solution and Bound to Liver Alcohol Dehydrogenase, Biochem., 15 (1976) 3165–3171.

[29] T. Yonetani and H. Theorell, On the Ternary Complex of Liver Alcohol Dehydrogenase with Reduced Coenzyme and Isobutyramide. Effect of p-Chloromercuriphenyl Sulfonate and Stability of the Complex, Archives Biochem. Biophys., 99 (1962) 433–446.

[30] J. Ridley and M. Zerner, Intermediate Neglect of Differential Overlap (INDO) Technique for Spectroscopy: Pyrrole and the Azines, Theor. Chim. Acta(Berl) 32 (1973) 111–134.

[31] P.R. Callis, Molecular orbital theory of the 1La and 1Lb states of indole, J. Chem. Phys., 95 (1991) 4230–4240.

[32] P.R. Callis, On the theory of two — photon induced fluorescence anisotropy with application to indoles, J. Chem. Phys., 99 (1993) 27–37.

[33] L.B. Clark, Electronic Spectrum of the Adenine Chromophore, J. Phys. Chem., 94 (1990) 2873–2879.
[34] S.A. Williams and P.R. Callis, Two-photon electronic spectra of nucleotides, Proc. SPIE–Int. Soc. Opt. Eng., 1204 (1990) 332–343.
[35] N.J. Oppenheimer, L.J. Arnold, Jr. and N.O. Kaplan, Stereospecificity of the Intramolecular Association of Reduced Pyridine Coenzymes, Biochem., 17 (1978) 2613–2619.
[36] G. Krishnamoorthy, N. Periasamy and B. Venkataraman, On the Origin of Heterogeneity of Fluorescence Decay Kinetics of reduced Nicotanamide Adenine Dinucleotide, Biochem. Biophys. res. Commun., 144 (1987) 387–392.
[37] M.A. Abdallach, J.-F. Biellmann, P. Wiget, R. Joppich-Kuhn and P.L. Luisi, Fluorescence Quenching and Energy Transfer in Complex Between Horse-Liver Alcohol Dehydrogenase and Coenzymes, Eur. J. Biochem., 89 (1978) 397–405.
[38] W.R. Lowes and J.D. Shore, The Mechanism of Quenching of Liver Alcohol Dehydrogenase Fluorescence Due to Ternary Complex Formation, J. Biol. Chem., 253 (1978) 8593–8597.
[39] W.R. Lowes and J.D. Shore, Spectral Evidence for Tyrosine Ionization Linked to a Conformational Change in Liver Alcohol Dehydrogenase Ternary Complexes, J. Biol. Chem., 254 (1979) 2582–2584.
[40] H. Eklund, J.-P. Samama and T.A. Jones, Crystallographic Investigations of Nicotinamide Adenine Dinucleotide Binding to Horse Liver Alcohol Dehydrogenase, Biochem., 23 (1984) 5982–5996.